ELSEVIER

PROGRESS IN NUCLEAR MAGNETIC RESONANCE SPECTROSCOPY

Progress in Nuclear Magnetic Resonance Spectroscopy 40 (2002) 175–197

www.elsevier.com/locate/pnmrs

NMR dipolar couplings for the structure determination of biopolymers in solution

Eva de Alba, Nico Tjandra*

Laboratory of Biophysical Chemistry, National Heart, Lung and Blood Institute, National Institutes of Health, Building 50, Room 3513, Bethesda, MD 20892, USA

Accepted 6 November 2001

Contents

Keywords: Nucleic acid; *J* coupling; Structure refinement; Protein; Liquid crystal

1. Introduction

There are several parameters derived from NMR data that have been traditionally used in the structure calculation of biological molecules such as peptides, proteins, oligosaccharides and nucleic acids. For example, information on dihedral angles can be obtained by the measurement of *J* coupling constants [1]. In addition, knowledge of the type of protein and peptide secondary structure is gained on the basis of the so-called secondary shifts [2,3]. This parameter is calculated as the difference between the experimentally observed chemical shift and the chemical shift of an unstructured molecule. Another example is given by the information derived from hydrogen exchange experiments, which is an indirect indication of the existence of hydrogen bonds. Recently, the measurement of *J* coupling interactions through hydrogen bonds has given direct evidence of their presence [4–6]. Nevertheless, the most important NMR

* Corresponding author. Tel.: +1-301-402-3029; fax: +1-301-402-3405.

E-mail address: nico@helix.nih.gov (N. Tjandra).

PII: S0079-6565(01)00042-5

parameter for structure determination is the nuclear Overhauser effect (NOE). The presence of a NOE crosspeak between two atoms implies that they are at a distance smaller than ~5 Å.

While chemical shifts and *J* coupling constants give local structure information, NOE data can relate atoms that are far apart in the series of chemical bonds connecting the biomolecule, but are close in space. Usually, structure calculation requires a large amount of NOE data. The typical qualitative interpretation of NOE information can lead to acceptable precise structures only because the inherent redundancy in the data. In spite of this, there are some cases where all the traditional NMR parameters fail to determine the three-dimensional structure. One example is when a protein is not globular and has several domains that are structurally independent. In this situation it is very difficult to determine the relative orientation of the domains, due to the sparse number of NOE crosspeaks connecting them. This problem is also present in the structure calculation of nucleic acids, where in addition to a low proton density, there is usually a lack of tertiary-type of structure, and therefore only medium- and short-range NOE contacts are observed. Mainly for this reason nucleic acid structures are often poorly defined.

Fortunately, a well-known NMR parameter called the dipolar coupling, that has not been particularly useful in the solution structure determination of biopolymers in the past, has recently occupied a very important place in this field [7–9]. In the case where two nuclei are scalar coupled, the dipolar coupling is manifested as an apparent addition to the *J* coupling when the molecule under study is anisotropically oriented in the magnetic field. The dipolar coupling is the physical response of the interaction between the magnetic dipole of two atoms and the external magnetic field. This type of interaction is always present when the molecule is under the influence of a magnetic field, but averages to zero by the isotropic tumbling of the molecule in solution unless this movement is restricted to a preferred direction.

The dipolar coupling has been measured in the past years in solution NMR using liquid crystals [10,11] and magnetic alignment [12]. Nevertheless, its utilization in biopolymer structure calculation has been impaired by the complexity of the spectra obtained, which resulted from the large degree of ordering achieved originally with liquid crystalline media. It has been shown recently that the use of dilute liquid crystals can create sufficient anisotropy for a small fraction of the molecules to adopt a preferred alignment direction in the medium [13,14], allowing residual dipolar couplings to be observed while the simplicity of the spectra is still conserved. Typically, the degree of order is such that the value of the static dipolar coupling is scaled down by a factor of at least 10^3. As we will discuss later, there are several methods to create dilute liquid crystals. At the present time, a considerable number of proteins, oligosaccharides and nucleic acids have been dissolved in this type of media and residual dipolar couplings have been used in their structure determinations.

Residual dipolar couplings have also been measured in the absence of any orienting media when the biomolecule has a sufficiently large magnetic susceptibility anisotropy to cause it to adopt a preferred orientation with respect to the external magnetic field [15]. This has been shown for both paramagnetic and diamagnetic biomolecules. In the case of paramagnetic proteins [16], the natural alignment with a high magnetic field is usually one order of magnitude smaller than that achieved by the use of orienting media. The same is true for nucleic acids [17], in which the almost perfect stacking of their bases dominates the susceptibility anisotropy. However, in general, the net alignment of diamagnetic biomolecules will be at least another order of magnitude smaller than that of their paramagnetic counterparts [18]. This fact renders the field alignment approach to be impractical for common NMR biomolecular structure application. Nevertheless, this method is still the only one in which residual dipolar couplings can be observed without incurring changes in the sample conditions.

In practice, the alignment tensor is defined by the traceless matrix *A*, which is equivalent to the Saupe matrix [10] if the liquid crystal director is parallel to the magnetic field, and has five independent elements (i.e. A_{ZZ}, $A_{XX} - A_{YY}$, A_{XY}, A_{XZ}, A_{YZ}. *XYZ* represents the molecular frame). A simple transformation that diagonalizes the tensor *A* also relates the molecular frame to the principal axis frame of the alignment tensor (x,y,z). In this later frame the dipolar coupling between two nuclei, P and Q, as a function of the

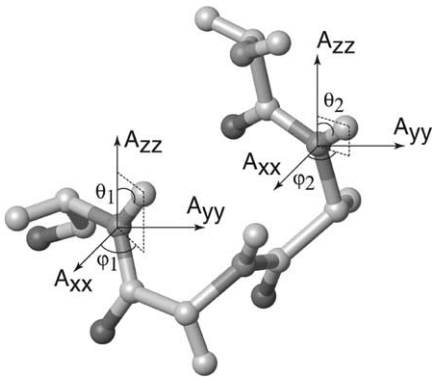

Fig. 1. Orientation of two dipolar coupling vectors in a protein segment. The vectors connect the amide $^{1}H^{N}$ and ^{15}N atoms. In this case the interaction vector coincides with the chemical bond. The axis system of the alignment tensor is designated as A_{xx}, A_{yy}, A_{zz}. The angles θ_1, φ_1, and θ_2, φ_2 define the orientation of both dipolar vectors with respect to the alignment tensor [7].

polar coordinates, θ and φ, is given by

$$D_{P,Q(\theta,\phi)} = D_a^{PQ}\{(3\cos^2\theta - 1) + 3/2R\sin^2\theta\cos 2\varphi\} \quad (1)$$

where

$$D_a^{PQ} = -(\mu_0 h/16\pi^3)S\gamma_P\gamma_Q\left\langle r_{PQ}^{-3}\right\rangle A_a \quad (2)$$

A_a is the dimensionless axial component of the alignment tensor, i.e. $A_{zz} - (A_{xx} + A_{yy})/2$, and $R = (A_{xx} - A_{yy})/A_{zz}$. S is the generalized order parameter [19]. γ_P and γ_Q are the gyromagnetic ratios of nuclei P and Q. μ_0 is the magnetic susceptibility. The polar angles θ and φ describe the orientation of the vector in the alignment tensor coordinate system (Fig. 1). r_{PQ} is the distance between atoms P and Q. In practice, the magnitude of the alignment tensor is defined by D_a (in Hz) which is commonly normalized to the value observed for NH dipoles.

In Eqs. (1) and (2), the presence of internal dynamics is taken into account by the order parameter S and the time averaging of the r_{PQ} distance, indicated by brackets. Several assumptions regarding internal motion are considered in order to obtain Eqs. (1) and (2). First of all, it is assumed that internal motion does not modify the overall alignment. This is an acceptable assumption when the internal motion is fast and its amplitude is small. In general, the fast motion of the internuclear vector can be described as an isotropic diffusion in a cone with a certain semi-angle. This type of averaging of the internuclear vector leads to the order parameter, S^2, commonly used in NMR relaxation studies [19]. Thus, angular averaging resulting from internal motion with respect to the alignment frame renders a dipolar coupling that is scaled down by the generalized order parameter **S**. Additionally, independent averaging of the r_{PQ} distance can be done under the assumption that vibrational motion is not coupled to librational motion.

Eq. (1) differs by a factor of 3/2 with respect to similar equations that relate the residual dipolar coupling to the components of the Saupe matrix. This factor comes from the relationship between the Saupe order parameters, expressed in a Cartesian molecular frame, and the alignment tensor components, which describe the deviation from the uniform distribution. A detailed explanation of how to obtain Eqs. (1) and (2) from the dipolar coupling hamiltonian can be found in the review by Bax et al. [9] and Prestegard et al. [8].

As can be noticed from the previous equations, the dipolar coupling value depends on the orientation of the vector connecting the two atoms with respect to the alignment tensor. Therefore, once the orientation of the alignment tensor, the dipolar coupling, and the distance between the two atoms are known, it is possible to derive the orientation of each vector with respect to a reference frame (Fig. 1). The position of the vector can be restricted into a cone about the principal axis of the alignment tensor (assuming it is axially symmetric). In the more general case of an asymmetric tensor the cone is distorted [20]. Since the alignment tensor is of second rank, and the direction of a second rank interaction is indistinct from its inverse, the dipolar coupling defines two cones of possible vector orientations. This ambiguity complicates the determination of local geometry in the absence of other structural information. Fortunately, it is possible to combine residual dipolar data obtained under anisotropic conditions where either the orientation and/or the rhombicity of the alignment tensor are different [20]. The angle at which the two cones intersect will indicate the orientation of the vector (Fig. 2). In Section 2 some of the procedures used to modify the alignment tensor will be discussed.

According to the explanations given earlier, the use of dipolar couplings makes possible the determination

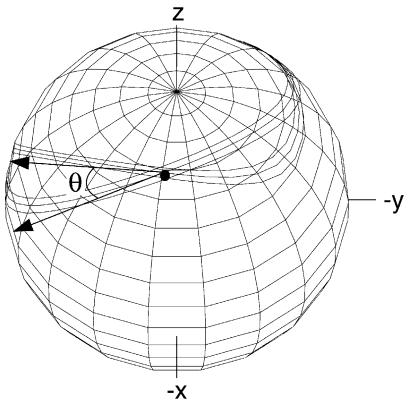

Fig. 2. Orientations of an amide N–H dipolar coupling bond-vector of the protein ubiquitin. Each cone of orientations is compatible with two different alignment directions adopted by the protein in two different alignment media. The inner lines correspond to the orientations obtained from the measured dipolar couplings. The outer lines include orientations that are possible if the dipolar coupling values are either increased or decreased by 1 Hz. The angle at which both cones intersect is defined by θ. The solid dot at the cone intersection determines the orientation of the dipolar coupling vector. (Reproduced with permission from Ref. [20]).

of the relative orientation of different domains in a multidomain protein, even if there are no NOE contacts between them. Analogously, the use of dipolar couplings greatly facilitates the structure determination of nucleic acids for similar reasons. The effect of the inclusion of dipolar couplings in the structure calculation of nucleic acids can be more substantial than in the case of proteins, since dipolar couplings can constitute up to 50% of the total structural data for the former, while only 10–15% for the later.

It has been demonstrated that the structural information provided by residual dipolar couplings greatly improves the accuracy with which structures are determined [21]. Nevertheless, residual dipolar couplings can be used for purposes other than biopolymer structure refinement. For example, structure validation factors have been defined in terms of dipolar couplings [22,23]. Another example is the use of residual dipolar couplings and ^{15}N NMR relaxation data to identify protein residues that undergo conformational exchange [24]. Additionally, dipolar couplings have been used to obtain information on ligand orientation in protein–ligand complexes, as well as to determine the global fold of proteins with

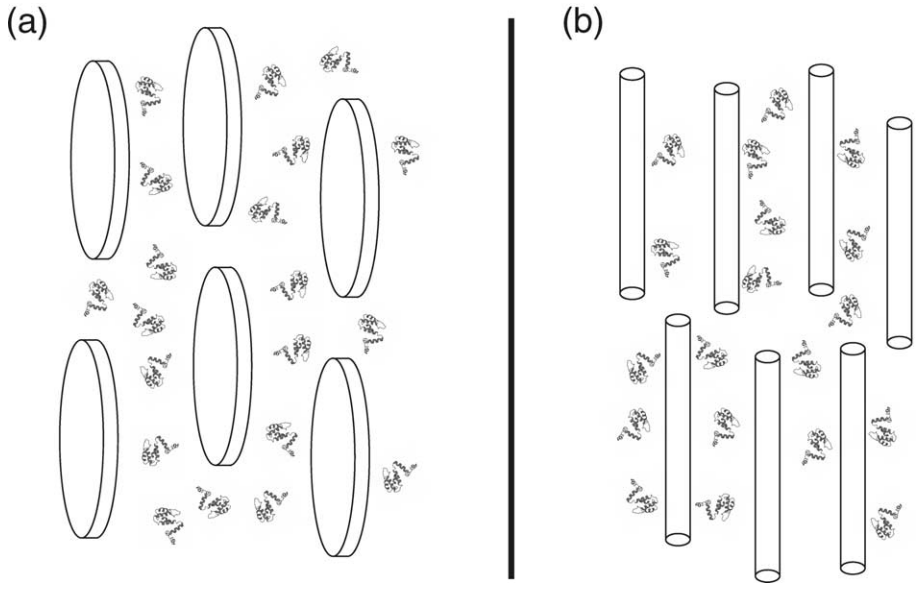

Fig. 3. Cartoon illustrating the alignment of the particles of two different orienting media [7]. (a) Disc particles represent lipid bicelles. (b) Rods represent viral particles. Bicelles orient with their normal orthogonal to the magnetic field [14] and viruses with their long axis parallel to it [33].

a low density of NOE data. These aspects related to the use of dipolar couplings will be discussed later.

In the following sections we will describe some of the reported methods used to orient biopolymers in solution, how to measure dipolar couplings and how to extract from their values the structural information. We will discuss different approaches used to interpret this structural information and to apply it into biomolecule structure calculations.

2. Orienting media

Biological macromolecules can be directly aligned in the magnetic field when they have sufficient magnetic susceptibility anisotropy, as mentioned above. Alignment in electric fields [25] and in liquid crystalline phases is also possible. This last method has been used extensively in the past to orient solutes in order to extract structural information. The liquid crystalline media that were typically used produced a very large degree of orientation. Therefore, for biopolymers, the observed NMR spectra were very complex due to the presence of long-range dipolar couplings, and too difficult to analyze. Some compounds have been discovered recently, which form dilute liquid crystals at low concentrations thus allowing a moderate degree of alignment. The first compounds used to study protein structure in weakly aligned states were dihexanoyl phosphatidylcholine (DHPC) and dimyristoyl phosphatidylcholine (DMPC), which undergo a gel to lyotropic liquid crystal phase transition at or above room temperature when mixed in solution [13]. This type of liquid crystal is formed by disc-shaped particles (bicelles) that are diamagnetic and orient in the magnetic field. Bicelle orientation in turn induces a slight alignment of the solute present in the medium via steric (in the case of neutral bicelles) [14] or electrostatic forces (in the case of charged bicelles) [20], creating in this way the necessary anisotropy to measure residual dipolar couplings (Fig. 3).

Modifications of these types of compound have been reported that have increased stability under strong acid and basic conditions, as well as over wider temperature ranges. For example, the carboxy-ester bonds present in DMPC and DHPC can be replaced by ether linkages, thus preventing acid or base catalyzed hydrolysis [22]. In addition, ternary mixtures of similar compounds allow the gel to liquid crystal phase transition to occur at different temperatures [26,27]. This may be an advantage for proteins that have low stability at high temperature, since the original bicelle method (DMPC/DHPC) has a temperature range for its liquid crystalline state that roughly goes from 35 to 45 °C [26]. Other novel bicelle systems composed of a mixture of 1,2-di-*O*-dodecyl-*sn*-glycero-3-phosphocholine and 3-(chloramidopropyl)dimethylammonio-2-hydroxyl-1-propane sulfonate have been designed to orient proteins at low pH values and over wide temperature ranges [28].

Orienting systems of quasi-ternary mixtures; cetylpyridinium chloride/hexanol/NaCl [29] and cetylpyridinium bromide/hexanol/NaBr [30] have been reported to form lamellar liquid crystalline phases that allow a large temperature range over which dipolar couplings can be measured. Similar mixtures of *n*-alkyl-poly(ethylene glycol)/*n*-alkyl alcohol and glucopone/*n*-hexanol have been shown to form lyotropic systems useful for biological macromolecule orientation in solution [31]. These components are less expensive than other alignment systems and commercially available. The main feature of these systems is that they have little, if any, binding capacity for macromolecules. They are uncharged, and thus are not affected by pH changes and little affected by salt, plus they tolerate large amounts of protein.

Another commonly utilized method to get a moderate degree of biomolecular alignment is by the use of filamentous viruses [32,33]. Once the virus particles reach a certain concentration in solution a nematic phase is formed. The viruses adopt a preferred orientation in the presence of the magnetic field that is transferred to the solute. Biological macromolecules have also been aligned using purple membrane preparations [34,35]. The purple membrane is formed by two-dimensional crystals of the membrane protein bacteriorhodopsin.

Suspensions of cellulose crystallites have proven to be a stable liquid crystalline medium for the measurement of residual dipolar couplings of biological macromolecules [36]. They seem to be particularly useful for highly charged molecules that interact with other orienting media. Another method to orient biopolymers consists in the use of a cross-linked

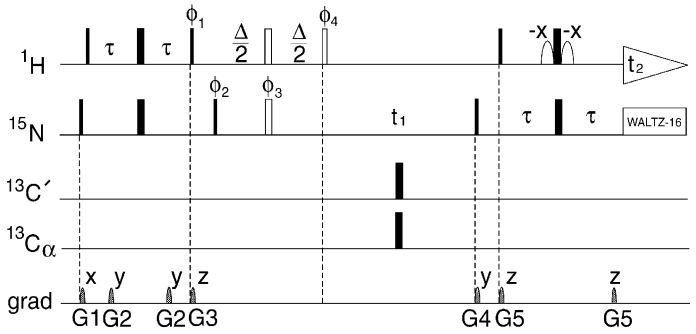

Fig. 4. Schematic representation of the pulse program IPAP-[^{1}H–^{15}N]-HSQC. Narrow and wide bars represent 90° and 180° pulses, with phase x unless indicated. The white bars represent pulses that are applied only when the anti-phase spectrum is acquired. The anti-phase and in-phase spectra are recorded in an interleaved manner. The WATERGATE solvent suppression scheme [106] is used at the end of the pulse program. 180° pulses are applied sequentially on C_α and C' to decouple ^{13}C from ^{15}N during nitrogen chemical shift evolution. $\tau = 2.5$ ms; $\Delta = 5.3$ ms. All gradients are sine-bell shaped of 25 G/cm at their center. Gradient durations: $G_{1,2,3,4,5} = 2$, 0.4, 2, 1, 0.4 ms. Phase cycling; $\phi_1 = -y, y$; $\phi_2 = 2(x), 2(-x)$ for in-phase and $\phi_2 = 2(-y), 2(y)$ for anti-phase; $\phi_3 = 4(x), 4(y), 4(-x), 4(-y)$; $\phi_4 = 8(x), 8(-x)$; receiver $= x, 2(-x), x$ for in-phase and receiver $= x, 2(-x), x, -x, 2(x), -x$ for anti-phase. Quadrature detection in the t_1 dimension is obtained by altering ϕ_2 for the in-phase and ϕ_2, ϕ_3 simultaneously for the anti-phase in the States-TPPI manner [107]. (Reproduced with permission from Ref. [44]).

polyacrylamide gel [37]. The protein enters the gel by diffusion from an external solution. The anisotropy in the gel is induced by straining it, either by compression or by stretching. The alignment is in this case independent of the magnetic field. A similar approach has been reported by Sass et al. [38], in which the alignment can also be achieved by embedding oriented purple membrane fragments in the gel.

As mentioned above, in the case of charged bicelles, the alignment of the protein is governed by both steric and electrostatic interactions. Thus, it is possible to modify the alignment by changing the type of protein–bicelle interaction or using different types of orienting media. Modulation of the alignment tensor has been reported in experiments in which either, the net charge of the bicelle or the sample pH has been changed, or a substantial increase in the net charge of the protein is created [20]. Additionally, two alignment tensors can be obtained using two different orienting media, such as bicelles and bacteriophages [39]. As commented earlier, the information derived from dipolar couplings of a biomolecule oriented in different directions is complementary and greatly improves structure quality.

It is noteworthy that one of the most important properties of all these media is that they are able to induce alignment through weak interactions of the solute with the liquid crystal. This way the rotational tumbling of the molecule will not be impaired or restricted and therefore no additional broadening of resonance lines, due to relaxation phenomena, will be observed [40].

3. Dipolar coupling measurements

For two nuclei that are scalar coupled, the presence of residual dipolar coupling will translate into a modification of the magnitude of the spin–spin coupling. Therefore, the difference between the splitting observed under anisotropic conditions (T_{PQ}) and the splitting observed under isotropic ones (J_{PQ}) provides the value for the residual dipolar coupling (D_{PQ})

$$T_{PQ} = J_{PQ} + D_{PQ} \tag{3}$$

Typically, five types of dipolar couplings are measurable in a protein. These are the one-bond amide NH, $C_\alpha H_\alpha$, $C_\alpha C'$, $C'N$ and the two-bond $H^N C'$. One-bond dipolar couplings are easier to interpret because the inter-atomic distance is known and the magnitude of the dipolar interaction is relatively large (Eqs. (1) and (2)). The NMR pulse programs most commonly used to measure the mentioned dipolar couplings are modifications of the ^{15}N-HSQC, ^{13}C-HSQC and HNCO experiments. These three NMR experiments allow J coupling evolution between the nuclei that give rise to the dipolar coupling at one stage of the experiment. For example, in the ^{15}N-HSQC experiment ^{1}H–^{15}N J

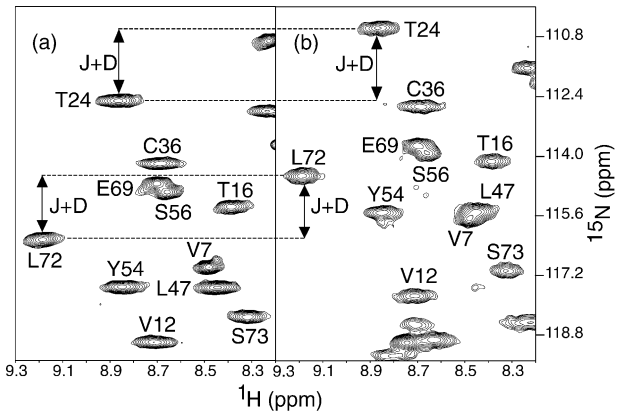

Fig. 5. Downfield (a) and upfield (b) components of ^{15}N doublets in the 600 MHz ^{15}N-HSQC spectrum of the protein saposin [108] in Pf1 viruses. (a) Results from the substraction and (b) from the addition of the in-phase and anti-phase spectra recorded with the IPAP-[^{1}H–^{15}N]-HSQC experiment, respectively. The sum of the residual dipolar coupling (D) and the J values can be obtained from the difference in frequency of the two components (arrows). The broad aspect of the signals indicates the presence long-range ^{1}H–^{1}H dipolar couplings.

coupling evolution is active when ^{15}N chemical shift is recorded. In this way amide dipolar coupling can be measured. J coupling evolution is recorded during the indirect dimension since transverse relaxation is slower in the ^{15}N dimension than in the ^{1}H dimension. If C′N coupling is active as well during the ^{15}N chemical shift evolution [41], this dipolar coupling can also be obtained.

The two-bond $H^{N}C'$ dipolar coupling is also observable in the ^{15}N-HSQC experiment. The doublet components of the ^{15}N are displaced one with respect to the other in the ^{1}H dimension as in an E.COSY experiment [42] due to this two-bond coupling.

An additional and very important feature of the ^{15}N-HSQC-type of experiments used to measure dipolar couplings is that they are spin-state selective. This selection can be achieved, either by storing separately the fraction of the ^{15}N magnetization doublet components formed by the ^{1}H–^{15}N J coupling that are in-phase and anti-phase [43], or by collecting the two doublets in different subspectra (IPAP method; for in-phase and anti-phase) (Fig. 4) [44]. These subspectra can be added and subtracted generating other spectra; one containing the upfield component of the doublet and the other containing the downfield component (Fig. 5). This method alleviates NMR signal crowding due to the presence of the coupling. For large proteins (i.e. proteins with rotational correlation times exceeding 15 ns) modified versions of the TROSY experiment [45] can be used to obtain the one-bond NH amide dipolar coupling. In cases where spectral crowding is very severe HNCO-based experiments allow the measurement of all or some of the four dipolar couplings (Fig. 6): NH, $C_{\alpha}C'$, C′N and the two-bond $H^{N}C'$ [46–50]. For example, a new method has been described recently to obtain accurate measurements of C′N dipolar coupling. The C′N coupling is derived from the relative intensity of two TROSY–HNCO spectra. One spectrum, in which the $J_{C'N}$ dephasing time is $1/2J_{C'N}$, is used as a reference. The other contains non-zero intensity resulting from the presence of the dipolar coupling, since the dephasing interval is set to $1/J_{C'N}$ [51].

One of the most commonly used pulse programs for the measurement of the $C_{\alpha}H_{\alpha}$ dipolar coupling is a J-modulated pseudo-three-dimensional version of the constant time ^{13}C-HSQC [52,53]. Coupling values are obtained from a time-domain fitting in the third dimension. This experiment is also used for the measurement of dipolar couplings of nuclei that belong to methyl and methylene groups. These last dipolar couplings have to be applied cautiously in structure calculation, since side chains are subject to conformational averaging that decreases the dipolar coupling from its expected value for a fixed conformation. Due to spectral overlap, which is very common in ^{13}C-HSQC experiments of proteins, sometimes only a few $C_{\alpha}H_{\alpha}$ dipolar couplings can be obtained with sufficient accuracy. In this situation

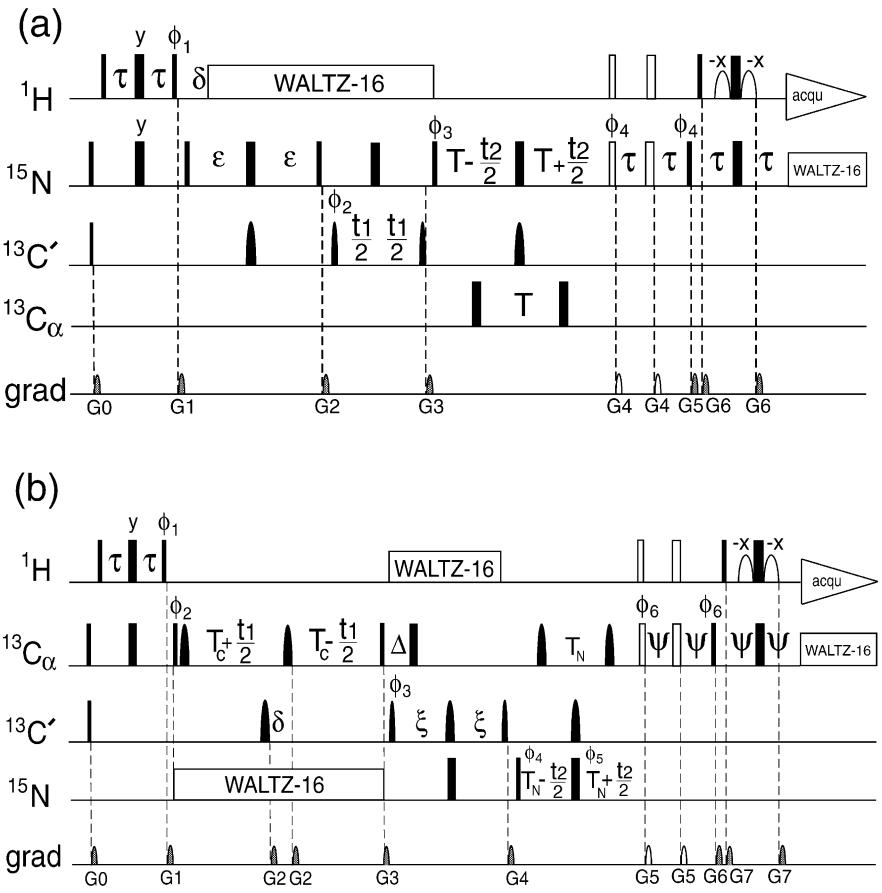

Fig. 6. Schematic representation of the pulse programs used for the modified version of the HNCO (a) and the (HA)CA(CO)NH (b) experiments. In (a), $\tau = 2.65$ ms, $\delta = 5.4$ ms, $\epsilon = 12.5$ ms, and $2T = 27.2$ ms. All pulses for which there is no specification of phase are applied in x. The phase cycling of the rest of the pulses is: $\phi_1 = y, -y$; $\phi_2 = 4(x), 4(-x)$; $\phi_3 = x$; $\phi_4 = 2(-x), 2(x)$; Receiver $= x, 2(-x), x, -x, 2(x), -x$. Quadrature detection in the ^{13}C and ^{15}N dimensions is achieved by States-TPPI [107] on ϕ_2 and ϕ_3, respectively. All gradients are sine-bell shaped with strength of 25 G/cm when applied on x or y and 35 G/cm on z. The durations of the gradients are: $G_{0,1,2,3,4,5,6} = 2.5$, 1.1, 0.7, 1.3, 1.0, 2.7, 0.4 ms, with respective gradient axes: yz, x, yz, xz, xy, yz, z. In (b), $\tau = 1.5$ ms, $\delta = 8.6$ ms, $T_c = 12.6$ ms, $\Delta = 4.5$ ms, $\xi = 13$ m, $2T_N = 29.6$ ms, $\psi = 2.65$ ms. The phase cycling is: $\phi_1 = y, -y$; $\phi_2 = x$; $\phi_3 = 2(x), 2(-x)$; $\phi_4 = x$; $\phi_5 = 4(x), 4(y)$; $\phi_6 = 4(x), 4(-x)$; Receiver $= x, 2(-x), 2(x), 2(-x), x$. Quadrature detection in the ^{13}C and ^{15}N dimensions is achieved by States-TPPI [107] on ϕ_2 and ϕ_4, respectively. The length of the gradients are: $G_{0,1,2,3,4,5,6,7} = 2.5$, 1.0, 0.7, 1.3, 1.2, 1.0, 2.5, 1.0 ms, and their respective axes are: yz, x, xyz, xz, y, xy, yz, z. For both Figures, narrow rectangular bars represent 90° pulses, while wide bars represent 180° pulses. Shaped pulses are represented by non-rectangular bars and are (sin x)/x in shape, except the second and third 180° pulses in C_α of (b), whose shape is hyperbolic-secant type with a squareness level of 3. The white bars represent the extra pulses that are applied in an interleaved manner to collect the in-phase ^{15}N magnetization. The anti-phase ^{15}N magnetization is collected without the application of the white pulses [50].

three-dimensional experiments such as HN(CO)CA or (HA)CA(CO)NH can be applied.

Since the value of the dipolar coupling depends on the gyromagnetic ratios and the inter-atomic distance, the intrinsic magnitudes of the $C_\alpha C'$ and the $C'N$ dipolar couplings are ~5 and ~9 times smaller than the NH dipolar coupling, respectively. And the magnitude of the $C_\alpha H_\alpha$ dipolar coupling is approximately two times larger than the one-bond amide dipolar coupling. One has to bear in mind these differences in order to have an estimate of the degree of accuracy with which to measure the different types of dipolar couplings and therefore, which NMR experiment to use for this purpose.

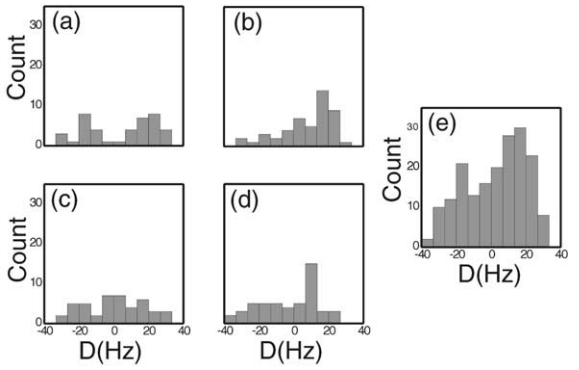

Fig. 7. Histograms of residual dipolar couplings observed for the C-terminal KH domain of the ribonucleoprotein K in 3.2% w/v bicelle solution [109]. (a) $^{1}D_{NH}$, (b) $^{1}D_{C\alpha H\alpha}$, (c) $^{1}D_{C'N}$, (d) $^{1}D_{C'C\alpha}$. None of each type of dipolar couplings properly represents a powder pattern. In contrast, a histogram that contains the addition of all normalized dipolar couplings provides a good representation of a powder pattern distribution (e).

The dipolar couplings that have been mentioned so far are heteronuclear and involve atoms that belong to the protein backbone. Homonuclear $^{1}H-^{1}H$ dipolar couplings can give very important structural information, not only because of the high density of protons in proteins but also because they can be very useful for the accurate determination of protein side chain conformations. Different types of NMR experiments can be used to determine the sign and magnitude of $^{1}H-^{1}H$ dipolar couplings [54–60]. Many of them are COSY-based heteronuclear experiments.

A more detailed description of the different aspects of this type of NMR experiments is reported in the review by Bax et al. [9].

4. Interpretation and use of dipolar couplings in protein structure calculation

4.1. Dipolar couplings for protein structure refinement

It is necessary to know a priori the magnitude and orientation of the alignment tensor in order to use dipolar couplings as structural restraints if no additional data is available in the structure calculation. In contrast, when using a set of NOE data together with dipolar couplings, only the magnitude of the alignment tensor needs to be known in advance. In this situation the orientation of the alignment tensor will be determined during the structure calculation process by treating it as a freely floating variable [21].

Very good estimations of D_a and the rhombic component of the alignment tensor R (Eq. (1)) can be obtained from the dipolar coupling values [61]. In the case of a uniform and isotropic distribution of dipolar bond-vectors the probability of finding dipolar coupling values between the extremes (vectors close to the z axis and vectors close to the y axis) has the same shape as a chemical shift anisotropy (CSA) powder pattern (Fig. 7). Due to the symmetric character of biopolymer structure, it is convenient to use more than one type of dipolar coupling to have a good estimation of D_a and R. For example, in the case of a protein whose secondary structure is mainly α-helical, all amide NH dipoles that belong to one of the helices will point to a similar direction. Therefore, the distribution of dipoles orientation will be very narrow and the powder pattern may not be well represented. This problem can be solved by using dipolar couplings of other pairs of backbone atoms. In order to do this the different types of dipolar couplings should be normalized with respect to one of them by taking into account the differences in the gyromagnetic ratios plus the bond distances between the atoms forming the dipole. All normalized dipolar couplings will be used to obtain the histogram with the powder pattern shape (Fig. 7).

Using this procedure the values of D_a and R can be obtained from Eqs. (4)–(7) [61]

$$A_{zz} = 2D_a \tag{4}$$

$$A_{yy} = -D_a(1 + 3/2R) \tag{5}$$

$$A_{xx} = -D_a(1 - 3/2R) \tag{6}$$

$$|A_{zz}| > |A_{yy}| \geq |A_{xx}| \tag{7}$$

In the recent work reported by Zweckstetter and Bax [62] an approach to determine the magnitude and direction of the alignment tensor is explained. This method is based on the molecular shape of the solute and uses a systematic search of solute orientations that have the highest tendency to clash with the orienting media. It works well provided that solute alignment is

driven only by steric interactions. The method is being modified to also consider electrostatic interactions.

In one of the reported methods for protein structure calculation [63] dipolar couplings are included as an empirical energy term added to the other conventional terms of the target function [21] (distances from NOE data, torsion angles, covalent geometry, etc.) used in a simulated annealing protocol. This equation takes the form

$$E_{\mathrm{dip}} = k_{\mathrm{dip}}(D^{\mathrm{calc}} - D^{\mathrm{obs}})^2 \tag{8}$$

where k_{dip} is a force constant, and D^{calc} and D^{obs} are the calculated and observed values of D, respectively.

E_{dip} is evaluated by calculating the angles that the bond-vectors form with a reference axis that is represented by a pseudomolecule located far away from the biopolymer. This pseudomolecule consists of four equidistant atoms (OXYZ). One represents the axis origin (O), the other three represent the three axis, OX, OY and OZ, which are orthogonal to one another. The pseudomolecule OXYZ reorients itself to yield the best fit between the calculated and the observed dipolar couplings. The force constant is chosen such that the errors between the predicted dipolar couplings from the calculated structure and the observed ones match the experimental errors.

Residual dipolar couplings can be incorporated into the structure calculation at any stage. Nevertheless, if applied once a preliminary structure is available from NOE data, dipolar couplings may help to identify misassigned NOEs and possible conflicts among the different types of data.

A method exists for applying dipolar couplings as restraints in structure calculation that does not require knowledge of the alignment tensor orientation with respect to the molecular reference frame [64]. With this method the projection angles between all pairs of internuclear vectors for which dipolar couplings are known have to be calculated. The calculation of these angles is done with respect to the molecular frame, therefore this method and the one which uses the orientation of the alignment tensor are very similar, although they differ in the mathematical expression of the dipolar coupling with respect to a chosen reference frame. Apparently, the former method also avoids convergence problems in the structure calculation that are present when using dipolar coupling values.

Another method of determining the magnitude and rhombicity of the alignment is based on the determination of the Saupe order matrix. Since it has five independent variables a minimum of five dipolar couplings have to be known. The anisotropic motional averaging parameter is represented by the Saupe matrix, which can be diagonalized by a transformation matrix that relates the principal frame in which the order matrix is diagonal to the initial molecular frame over which the dipolar couplings are defined. Singular value decomposition is the method proposed for determining the Saupe order matrix [65]. Using this method the values of D_{a} and R can be obtained provided that a good local structure of a molecular fragment is known, even when only a few dipolar couplings are available.

Dipolar couplings are affected by the fast internal motion of the protein and also by slow conformational averaging. Internal motion is taken into account by the generalized order parameter **S**. This parameter has a relative uniform value in the range 0.85–0.95 for a protein backbone that adopts a regular secondary structure. In contrast, other more mobile regions of a protein will have residual dipolar couplings reduced due to the fluctuations of the dipole with respect to the alignment tensor. Without any precise information on the amplitude of these large fluctuations dipolar couplings can still be used in structure refinement, provided that the obtained values are considered as a lower limit. Conformational averaging is more complicated to address. Firstly, the various conformations that may be present can orient differently with respect to the magnetic field. Secondly, when the conformational change involves a large part of the structure there is a good chance that the overall alignment tensor will be modified. In the absence of knowledge of the possible conformations that exist and the time scale involved, conformational averaging would be very difficult to take into account in structural studies that include dipolar coupling information.

Although protein backbone dipolar couplings are the most frequently used in structure calculations, it is also possible to measure this parameter in side chains. This has been done for methylene and methyl sites and the values obtained have been used in protein structure refinement [53]. In the case of methylenes the sum of both $C–H_1$ and $C–H_2$ dipolar couplings is obtained and the energy function that is minimized

has the form

$$E_{\mathrm{dip}} = k\left[\left(D^{\mathrm{cal}}_{\mathrm{CH1}} + D^{\mathrm{cal}}_{\mathrm{CH2}} - D^{\mathrm{obs}}_{\mathrm{CH1}} - D^{\mathrm{obs}}_{\mathrm{CH2}}\right)\right]^2 \qquad (9)$$

where D^{cal} and D^{obs} are the calculated and observed dipolar couplings, respectively.

In a side chain with a C–CH_3 moiety, rapid rotation of the methyl group makes the C–H dipole to appear to be located in the direction of the C–C bond, and scales the real value of the C–H dipolar coupling by a factor of $\sim -1/3$. Assuming that the C–C bond forms an angle of 0° with the z axis of the alignment tensor, the C–H bond forms an angle of ~109° with the C–C bond for a tetrahedral carbon atom. Typically for methyl groups the dipolar splitting that is measured accounts for three protons. This fact, together with the scaling factor that has been mentioned, results in a measured quantity that coincides in magnitude and is opposite in sign to a C–H dipolar coupling of a C–H dipole located in the C–C bond.

Due to the effect of fast conformational averaging on dipolar couplings of atoms that belong to protein side chains, their incorporation into structure calculation must be done carefully. In the absence of quantitative information regarding side chain motion and conformational averaging, it is assumed that the observed dipolar couplings provide lower limits on the magnitude of the real couplings. A proper way to take this into account is to apply a penalty function with the shape of a half-open square well. This same approach is also applied when incorporating backbone dipolar couplings of residues that undergo large amplitude fast motions into the structure calculation.

In the case of ^{1}H–^{1}H dipolar couplings, except for methylene groups, the distance between the protons is unknown. This variable, which is fixed for one-bond heteronuclear dipolar couplings, is included in the energy term represented by Eq. (10) [66]. When the sign of the ^{1}H–^{1}H dipolar coupling cannot be determined the calculation is carried out only against its magnitude. The energy term then takes the form

$$E_{\mathrm{dip}} = k(|D^{\mathrm{cal}}| - |D^{\mathrm{obs}}|)^2 \qquad (10)$$

As mentioned previously, a preliminary structure calculated with NOE data is commonly used in the refinement procedure that incorporates dipolar coupling information. Another approach used to obtain a starting model for the refinement is called molecular fragment replacement (MFR) [67]. This method treats the protein of interest as overlapping fragments of 7–10 residues in length. A protein database is used to find those fragments for which there is a best fit to the measured dipolar couplings. The average backbone angles of the best fragments are used to build the initial model. The MFR method will be explained in more detail in Section 4.5. Also in Section 4.5 another method is described for incorporating dipolar coupling data into protein structure calculation that is based on the orientation of peptide planes [68,69].

4.2. Dipolar couplings as protein structure validation factors

The use of residual dipolar couplings in protein structure calculation improves structure quality by reducing the dispersion of the ensemble of structures that satisfy all experimental restraints. Additionally, dipolar couplings allow the calculation of more accurate structures. This means that the calculated structures are closer to the 'real' one.

A structure quality factor (Q factor) that depends on dipolar coupling data and is analogous to the R factor used in X-ray crystallography [70] and in NMR [71] has been reported [22]. This factor describes the agreement between the calculated structure and the experimental data. The characteristics of the alignment tensor, such as its magnitude, rhombicity and orientation can be modified by changes in the experimental conditions. It is necessary to take this into account when comparing predicted versus measured dipolar couplings.

The Q factor is defined as follows:

$$Q = \left[\sum_{i=1,\ldots,N} (D^{\mathrm{obs}} - D^{\mathrm{cal}})^2/\mathrm{N}\right]^{1/2} /D^{\mathrm{rms}} \qquad (11)$$

where D^{obs} and D^{cal} are the experimentally measured and the predicted dipolar couplings. The summation extends over N residues for which dipolar couplings are known. D^{rms} is the root mean square value of dipolar couplings when these are randomly distributed and using an alignment tensor obtained from the best fit between the experimental data and the existing structure. If the distribution cannot be considered

uniform, D^{rms} may be calculated as [23,72]

$$D^{rms} = \left\{D_a^2[4 + 3(D_r/D_a)^2]/5\right\}^{1/2} \quad (12)$$

D_a and D_r are the axial and rhombic components of a traceless second rank diagonal tensor related to the alignment tensor.

Q has to be calculated for a set of restraints not used in the structure refinement. In this sense it is similar to the free R factor [70,73]. Q is very sensitive to small changes in structure and values of this factor that are smaller than 30% still indicate a good agreement between the calculated coordinates and the real structure.

Not only dipolar couplings can be used to define structure validation factors. Another NMR parameter, the CSA, has been utilized for this purpose as well [74]. There is a change in the chemical shift of nuclei between isotropic and anisotropic media. The chemical shift change is related to the orientation of the CSA tensor with respect to the alignment tensor. Another reported structure validation factor uses ^{15}N backbone relaxation rates to demonstrate the better quality of structures refined with residual dipolar couplings [75]. It is worth noting that most Q factors are calculated using data obtained under anisotropic conditions. Therefore, they do not reflect any possible structural changes derived from the presence of the orienting particles in the system. So far such an effect has not been reported but it is still prudent to bear it in mind. Only the Q factor that depends on the ^{15}N backbone relaxation rates is measured in isotropic conditions, thus it may be used as a way to indicate structural changes caused by the presence of the orienting media.

A different way of assessing structure quality is reported in the work by Nikolai et al. [76]. The authors translate dipolar couplings into angular restraints and use them to build consistency maps. These maps are utilized to examine the quality of protein structure.

4.3. Dipolar couplings in protein domain orientation

When protein domains have fixed orientations with respect to each other, determining the domain orientation using residual dipolar couplings is in practice and in concept similar to the structure refinement process that we have commented on above. This is so because a unique alignment tensor will represent the preferred orientation of both domains in the anisotropic environment. There are several reported works in which the importance of dipolar couplings in orienting fixed protein domains has been demonstrated, specially in cases with conformational ambiguity due to lack of NOE contacts between the domains. One example is the determination of subdomain orientation of the ribosomal protein S4 Δ41 [77]. In this work the lack of NOE contacts between the domains produces an ambiguity in interdomain orientation. The authors use two different anisotropic media to obtain dipolar couplings (DMPC/DHPC bicelles and Pf1 filamentous bacteriophages). They conclude that subdomain orientation in solution is similar to the one present in the crystal structure. In this case changes in subdomain orientation may explain how the protein recognizes RNA targets. This is an example of the importance in defining the relative domain conformation in solution, since the function of many multidomain proteins involves interdomain reorientation. Another example that, instead of using liquid crystal-induced alignment, utilizes magnetic alignment to obtain dipolar couplings, is the partial replacement of Ca^{2+} in Ca-binding proteins by a paramagnetic lanthanide ions such as Tb^{3+}. A study of this type has been performed with the fixed domains of calmodulin bound to a target peptide and the independently oriented domains of free calmodulin [78]. The Tb^{3+} ions bound to one calmodulin domain increase the magnetic susceptibility anisotropy of the protein, whose interaction with the external high magnetic field produces molecular alignment, and thus the presence of residual dipolar couplings. The degree of alignment of the domain that binds the lanthanide depends on its orientational freedom with respect to the other domain in free (not bound to the peptide) calmodulin. In addition, the paramagnetic Tb^{3+} ion creates a local magnetic field that produces shifts in the resonances of nuclei in the domain that does not bind to Tb^{3+} ions. Therefore this effect, known as the pseudocontact shift, depends on the orientation of one domain relative to the other and can be used as an indicator of the average orientation of both domains.

An additional reason why it is interesting to determine the relative domain orientation in solution is because there exists the possibility that domain conformations determined by X-ray crystallography

can be biased by the presence of crystal packing forces, and therefore may differ from the physiological relevant structure in solution. A difference between the X-ray and the solution structure of the maltodextrin-binding protein (MBP) loaded with β-cyclodextrin has been found using dipolar couplings obtained under a weakly aligned medium [79]. The solution conformation of this 370-residue protein has been obtained from the X-ray structure using a large set of dipolar couplings. Hinge-rotations have been applied to various crystal structures searching for the minimum difference between the experimentally measured and calculated dipolar couplings. The situation is somewhat different to the examples commented on before, since in this case orientational freedom between the domains is considered. Each domain will have a different average orientation with respect to the magnetic field, and therefore the residual dipolar couplings of residues belonging to each domain will have to be analyzed using two distinct alignment tensors. The calculated alignment parameters for the two domains of MBP are very similar. Nevertheless this evidence is not enough to rule out the presence of interdomain dynamics, since both domains can undergo the same amount of motion. In this study interdomain motion has been taken into account using three different models. In the first model it is assumed that there is a rapid exchange between an opened and a closed form of the protein. Since there is no significant improvement in the fitting of the measured dipolar couplings by using a two-state model, the authors conclude that the calculated solution structure accurately represents the average effective conformation. A second model considers multiple conformational species. It is assumed that the system can be described with a unique set of alignment parameters. According to the results interdomain dynamics modify the alignment parameters but do not affect the structural ones. In the third model the N-domain of MBP is mobile. The results obtained indicate that the motion does not translate into a change in the determined structure.

This method based on crystal structures has been used to analyze the dipolar coupling data of T4 lysozyme in the work reported by Goto et al. [80]. Once again the average solution conformation of this protein with two domains differs from the crystal structure in the relative orientation between both domains. The authors claim that crystal packing interactions can have an effect on protein domain orientation. This effect can be identified with the use of dipolar couplings.

Another example of the determination of the relative conformation of protein domains using dipolar couplings is the work reported by Fischer et al. [81]. The authors have studied the structure of a two-domain fragment of the barley lectin protein (BLP), for which two alignment tensors have been defined separately, one corresponding to each domain. This study indicates that BLP interdomain orientation differs from that present in the crystal structure of a highly homologous protein (approx. 95% identical in sequence). The differences between the alignment parameters of the two domains suggest that both can be considered to reorient independently.

4.4. Information about ligand conformation and orientation from residual dipolar couplings

Ligand conformation in protein–ligand complexes can reveal important information concerning protein function and can be used as a basis for rational drug design. X-ray crystallography and NOE based NMR techniques are the most common methods used to obtain this type of information. Nevertheless, determining the conformation of ligands using NOE data can be difficult due to the small number of NOE contacts between the protein and its ligand, which is a consequence of the, sometimes, large internuclear distances. Recently reported works have used residual dipolar couplings to extract information about ligand structure when ligands are bound to proteins. One example is the study by Bolon et al. [82] of a 149-residue fragment of the mannose-binding-protein-A (MBPA) bound to α-methyl mannoside (AMM). The authors have measured one-bond $^{1}H-^{13}C$ dipolar couplings in AMM when it is bound to MBPA in an orienting liquid crystal. The measured dipolar couplings are a weight average of the dipolar couplings of AMM in the free and in the bound states. The dipolar couplings of AMM in the orienting media but in the absence of MBPA are used as reference for the free state. The different pattern of dipolar coupling values in free AMM indicates that the magnitude and orientation of the AMM alignment tensor is modulated by the presence of MBPA and those values

are used to calculate the dipolar coupling when the AMM is bound to MBPA. In this study the orientational tensor of the protein is defined by the protein symmetry and the ligand orientational tensor is determined on the basis of the dipolar couplings. The superimposition of both tensors indicates the orientation of AMM with respect to the protein.

Residual dipolar couplings have been measured for a transducin peptide that transiently binds to rhodopsin in field-oriented rhodopsin-containing disks [83]. The binding is triggered by rhodopsin light-activation. The authors measure an increase in ^{15}N relaxation rates after activation, an increase in proton amide line width, as well as residual dipolar couplings and ^{15}N CSA. These data indicate that order is transferred from the oriented disks to the bound peptide. The angles that some of the peptide NH bond-vectors form with the magnetic field are obtained using dipolar coupling values. This work is an example of the conformational information that can be extracted on the basis of residual dipolar couplings for ligands bound into integral membrane receptor proteins. The current limitation of the method is that ligands must bind in the millimolar range.

4.5. Structure building using dipolar couplings in the absence or with sparse number of NOE data

Several attempts have been reported recently to define protein global folds in the absence or with a small number of NOE data. Considerable improvement in precision and accuracy of NMR structures have been obtained for the B1 domain of streptococcal protein G (GB1), the monomer of the barrier-to-autoregulation factor (BAF) and cyanovirin-N (CVN) when including dipolar coupling in protein structure calculation using a minimal number of NOE distance restraints [72]. In the case of GB1, since approximately 90% of the residues belong to secondary structure elements, only distance information derived from hydrogen bonds has been used together with dipolar couplings to successfully determine the overall fold. The accuracy, evaluated as resemblance of the structures calculated this way with the crystal structure, was improved. In contrast, in the case of BAF and CVN, NOEs connecting backbone to side chain and side chain to side chain were also included in the calculation.

Another example concerns the three-dimensional structure determination of Cytochrome c' [84]. This protein has a paramagnetic center and therefore different types of conformational restraints can be derived from this feature. In this case the authors have used structural information from pseudocontact paramagnetic chemical shifts, Curie-Dipolar cross-correlation, secondary structure constraints, as well as dipolar couplings and ^{15}N relaxation data of the anisotropically tumbling molecule. Dipolar couplings do not average to zero due to the susceptibility tensor anisotropy of the protein and no orienting media has been used. The structure calculation of the protein follows basically two steps. In the first place, only vectors or nuclei present in previously known elements of secondary structure are constrained. In the course of this calculation the magnitude and orientation of the magnetic susceptibility and rotational diffusion tensors are determined. Initial estimates of the values of the different components of these tensors are calculated using the method previously commented on concerning the powder pattern shape (vide supra). Nevertheless, the authors demonstrate that the success of their calculation protocol is largely independent of the initially estimated tensor values. In the second place, structures calculated in the first stage are refined using data from the loop regions, including only those residues with negligible internal dynamics. Structures calculated in each of the two steps are selected according to their energies. For the case studied, there is a difference in energy between the converged and the non-converged structures of 10% of the total target function. The authors conclude that the amount and quality of the structural information determines whether the structure calculation method will work properly and that their data are at the limit for obtaining good results. This protein structure determination without NOE data gives a root mean square deviation (RMSD) of 0.73 ($\pm$0.18) Å for the backbone atoms of the helical residues. The differences between these regions and the equivalent ones in the existing crystal structure is 1.7 Å. As the authors suggest, this method can be applied to a large number of metal-binding proteins, or to proteins capable of binding peptides containing lanthanide ions. For these cases, the structure of the protein should be unmodified by the change in the type of bound

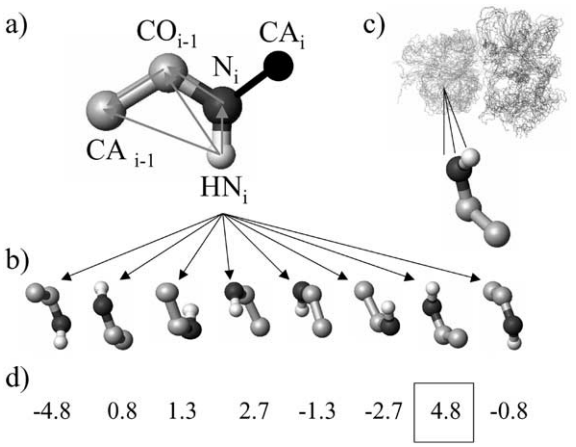

Fig. 8. (a) Dipolar coupling vectors represented by arrows for which residual dipolar couplings are measured. (b) Eight possible peptide plane orientations are compatible with the measured dipolar coupling data. (c) The correct peptide plane orientation is selected on the basis of the comparison between the eight orientations and the peptide plane of the average structure determined by the use of NOE and other structural data. (d) Sum of the dot product between the dipole vectors of each peptide plane and the corresponding vectors of the average plane. The results indicate that the peptide plane above the rectangle is the correct one. (Reproduced with permission from Ref. [68]).

metal and the paramagnetic center should stay static with respect to the protein.

Dipolar couplings have also been used to determine the global fold of the MBP (42 kDa) complexed with β-cylodextrin in the presence of a limited set of NOE restraints [68]. The authors use amide to amide, as well as amide to methyl and methyl to methyl distance restraints from NOEs. Structural information from hydrogen bonds and dihedral angles is also used. Initial structures are calculated with these restraints in the absence of dipolar coupling information. A global pair-wise backbone RMSD of 5.5 Å was obtained for these preliminary structures, which were then refined against residual dipolar couplings resulting in a large number of dipolar restraints violations. The authors suggest that the large number of dipolar coupling violations is due to the infinite number of orientations consistent with each dipolar coupling and the rest of the data. Therefore, the energy surface of the refinement process becomes very complex. For this reason, the authors develop a new protocol for the use of dipolar couplings in the calculation of large protein structures with a small set of NOE data. Their approach consists in orienting peptide planes using dipolar coupling data. Five dipolar couplings for each peptide plane are necessary to overdetermine the three degrees of freedom related to the three Euler angles that describe the transformation from the coordinate to the alignment frame, assuming that the axial and the rhombic components of the alignment tensor are known. The three Euler angles are determined by minimizing the difference between the predicted and the measured dipolar couplings. Eight possible orientations are obtained through this procedure (Fig. 8). The real orientation is chosen according to the preliminary structures that were calculated with the NOE, dihedral and hydrogen bond data. Direct refinement of NMR structures against residual dipolar couplings restricts vector orientation to a pair of cones in the case of an axially symmetric alignment tensor. In contrast, with the method proposed by these authors each vector is restrained into a well-defined value. Global pair-wise RMSD of MBP backbone is reduced from 5.5 to 2.2 Å with the inclusion of dipolar coupling restraints. Analogously, the RMSD to the existing crystal structure decreases from 5.1 (without dipolar data) to 3.3 Å (with dipolar data). This is another example of the increase in both the precision and the accuracy of the determined NMR structures with the use of dipolar couplings, even in the presence of a small number of NOE distance restraints.

A very different approach from the ones commented on above to define global folds in the absence of NOE data uses dipolar couplings, chemical shifts and a protein database with crystal structures of high resolution. The method is called molecular fragment replacement and has been applied to the protein ubiquitin [67]. MFR selects from the database those fragments of 7–10 residues whose predicted dipolar couplings best fit the set of measured ones, as well as the fragments with the smaller differences between the measured and calculated chemical shifts. The method gives less weight to the chemical shift selection. Average values of the ϕ and ψ angles of the selected fragments are calculated and used to build initial models that have an average RMSD of 6.95 Å with respect to the crystal structure. These preliminary structures can be subsequently refined by minimizing the difference between the measured and the calculated dipolar couplings, and analogously with

the chemical shifts. The refined structures have an RMSD of 0.88 Å with respect to the crystal structure.

In addition, docking of protein–protein complexes has been accurately performed using dipolar couplings and intermolecular NOEs [85]. For this method to work properly, high resolution structures of the free proteins have to be known and no significant backbone conformational changes must occur upon complexation. The docking is achieved by rigid body minimization using a target function that takes into account intermolecular NOEs, amide residual dipolar couplings and a purely repulsive intermolecular potential. Using dipolar couplings exclusively, with the absence of NOE data, there exists ambiguity concerning several possible orientation of one molecule relative to the other. The translational and orientational information contained in the NOE data help to solve this ambiguity. The effectiveness of the method is more clearly demonstrated when docking the complex in the presence of dipolar couplings and with a scarce number of NOEs. In this case, not only the lack of NOE information but also the limited precision and accuracy of NOE data is alleviated by the inclusion of dipolar coupling restraints, resulting in a rapid and accurate determination of the protein–protein complex structure.

4.6. Protein family search via dipolar couplings

Residual dipolar couplings have been used to recognize protein folds in the pioneer work of Annila et al. [86]. The idea is based on the secondary structure composition of proteins and its arrangement in a limited number of relative orientations. In this sense, backbone dipolar couplings measured for a protein of unknown structure can be compared to predicted dipolar couplings of proteins of known structure that compose a database in the search for a common fold. The authors of this work measure the amide residual dipolar couplings of a protein of undetermined structure named calerythrin, an EF-hand containing protein, and compare them to the calculated values of proteins that are members of the EF-hand family. The comparison indicates that calerythrin has a similar fold to proteins belonging to this family. It is important to note that calerythrin shares lower that 30% sequence homology with any of the proteins included in the database. In addition, the proteins within the EF-hand family have different types of folds.

In the case of proteins of resemblance to calerythrin the axial and rhombic components of the alignment tensor estimated from the measured dipolar couplings are used for the prediction. For proteins whose structure is suspected to be dissimilar to that of calerythrin, the use of those axial and rhombic tensor components can be a source of differences between the measured and the calculated dipolar couplings. Therefore, a minimization procedure was applied in which the smallest discrepancy between the experimental and the predicted values is searched allowing the directions of the alignment tensor to vary.

Within proteins of homologous structures the length of secondary structure fragments can vary considerably. This fact, as well as the presence of loops connecting the different elements of secondary structure, complicate the comparison between the experimental and the calculated dipolar couplings. Therefore, the authors suggest making an alignment of primary structures based on amino acid sequence homology, an alignment of secondary structure based on C_α secondary shifts and also about protein function if known, before comparing dipolar couplings. In the case reported by Annila et al. [86], the similarity between the measured dipolar couplings of calerythrin and two other proteins of the database is evident and unambiguous. In contrast, there is a clear discrepancy between the experimentally measured and the predicted values of calerythrin and the rest of the EF-hand family of proteins. Additionally, the authors find that the recognition of similar and dissimilar structures is independent of the uncertainties in the values of the axial and the rhombic components of the alignment tensor. The distribution of the errors squared between the measured dipolar couplings and the predicted ones also serves to identify similar or different folds. For example, for proteins whose structures are close, the dipolar couplings are very similar for the majority of the residues while only a few show large deviations. This can be explained if one considers that the agreement is located in the secondary structure fragments and dissimilarities concentrated in turns. This implies that it will be easier to recognize common folds when comparing proteins composed mainly of regular secondary structures. In contrast, for structures that are very different large deviations

are frequent. Related examples of the application of these ideas have been reported by Meiler et al. [87] and Fowler et al. [88] for the proteins rhodniin and NodF, respectively.

Dipolar couplings have also been used to validate models built by sequence homology methods. In addition, dipolar couplings have been shown to reduce the RMSD between these models and the target structure. The RMSD of sequence homology models of the protein calmodulin built from the structure of recoverin and parvalbumin has been reduced using heteronuclear dipolar couplings [89].

5. Interpretation and use of dipolar couplings in nucleic acid and oligosaccharide structure calculation

5.1. Dipolar couplings in the structure calculation of nucleic acids

The structure determination of nucleic acids by NMR methods tends to be difficult due to the absence of a globular fold and the low number of long-range NOEs that can be measured. As a result, the local geometry and the overall shape of the molecule are usually poorly defined. The incorporation of the 'long-range' information that dipolar couplings provide is expected to improve the quality of nucleic acid structures substantially [90]. In fact, residual dipolar couplings have been successfully applied in the structure calculation and structure refinement of DNA and RNA [91–95].

Bacteriophages constitute the orienting media that has been found to be more suitable for nucleic acid dipolar coupling measurements because similarity in the charges will reduce non-specific interactions. Nevertheless, it is equally possible to use neutral bicelles and in this case primarily steric interactions will drive the alignment. The type of dipolar couplings that can be measured for nucleic acids are $^{1}H-^{15}N$, $^{1}H-^{13}C$, $^{13}C-^{13}C$, $^{1}H-^{1}H$, and $^{1}H-^{31}P$. Due to rapid exchange of imino protons with water the number of measured $^{1}H-^{15}N$ dipolar couplings is usually small. In addition, $^{1}H-^{13}C$ dipolar couplings may be difficult to obtain due to spectral overlap in the aromatic and the sugar regions. This problem can be alleviated using selective labeling. Unless a previously determined structure is used, $^{1}H-^{1}H$ distances are not known a priori. Therefore, the angle as well as the distance of the dipolar vector have to be considered variable during the refinement process.

In the absence of the most common orienting media, such as bicelles and bacteriophages, paramagnetic ions have helped in the magnetic alignment of DNA in order to measure dipolar couplings. In the work reported by Berger et al. [96] paramagnetic europium ions bind to the narrow grooves of a DNA pentadecamer increasing the alignment relative to that observed for free DNA. The electron relaxation time of europium ions is relatively short and their effect is to shift NMR signals more than broadening them. This increase in the magnetic alignment allows the authors to measure $^{1}H-^{13}C$ residual dipolar couplings up to 70 Hz. The procedure to define the position of the alignment tensor consists again in a minimization of the difference between the predicted and the observed dipolar couplings. In the case of nucleic acids it is less reliable than in the case of proteins to estimate the magnitude and rhombicity of the alignment tensor from the distribution of the measured dipolar couplings, since the assumption of a uniform distribution of bond-vector orientations is far from real. In this work, the order parameter S^2 of all internuclear vectors is assumed to have a value of unity for the determination of the alignment tensor orientation. Isotropic diffusion on the surface of a cone is used as a model to take into account molecular motion. Nevertheless, the authors claim that the position of the alignment tensor does not seem to be highly sensitive to this motion.

The first RNA structure that has been refined using dipolar coupling information is part of a protein–RNA complex [92]. Previously determined structures of the complex without dipolar couplings were used as starting structures and refined using dipolar couplings measured for the protein and the RNA moiety. The authors of this work use an X-PLOR refinement protocol that has been optimized to refine protein structures with dipolar coupling restraints. It is known that protein refinement protocols do not operate well for RNA structures. In this case, using previously calculated structures in the absence of dipolar data, the authors tested the performance of the protein-optimized refinement method and found that the overall RMSD remains

Restrained molecular dynamics protocol

1) Randomization

Total time: 16ps
Temperature: 1000K
Energy terms: bonds, angles, improper torsions
Number of calculated structures: 40

2) Global fold

a) 500 cycles of energy minimization
Energy terms: bonds, angles, improper torsions
b) 15ps of restrained molecular dynamics
Energy terms: bonds, angles, improper torsions, NOE
Soft-square NOE potential
k_{NOE} = 50kcal/mol Å^2
Step size: 1fs
Temperature: 1000K
c) 200 steps of energy minimization
d) Restrained molecular dynamics
20 cycles of 1ps each
Energy terms: bonds, angles, improper torsions, NOE, van der Waals (Lennard-Jones)
van der Waals repulsion energy is increased by a factor of 1.23, from 0.0015 to 0.1
Step size: 1fs
Temperature: 1000K
e) 200 steps of energy minimization
f) Restrained molecular dynamics while cooling to 300K
28 cycles of 0.5ps each
Temperature increment: 25K per cycle
Step size: 1fs
Energy terms: bonds, angles, improper torsions, NOE, van der Waals (Lennard-Jones)
g) 1000 cycles of energy minimization

3) Refinement

a) 500 cycles of energy minimization
Energy terms: bonds, angles, improper torsions, NOE, van der Waals (Lennard-Jones)
Soft-square NOE potential
k_{NOE} = 50kcal/mol Å^2
k_{DIH} = 5kcal/mol rad^2
b) 2.5ps of restrained molecular dynamics while increasing the force constants of the $\beta, \gamma, \delta, \varepsilon$ torsion angles
k_{NOE}: from 1 to 50kcal/mol Å^2, increased by a factor of 1.22 per cycle

Fig. 9. Schematic representation of the protocol used in the structure calculation of a DNA dodecamer using residual dipolar couplings [97].

essentially unchanged, although the sampling of the conformational space by the protocol optimized for RNA structures seems to be more exhaustive. As a result of the refinement process, the relative position of the two double helical RNA stems is better defined. In contrast, the precision of the refined structures does not improve with respect to the unrefined ones.

In the work reported by Tjandra et al. [97], the structure of a DNA dodecamer is calculated using

k_{DIH}: from 1 to 200kcal/mol rad^2, increased by a factor of 1.30 per cycle
Step size: 0.5fs
Temperature: 1000K

c) 2.5ps of restrained molecular dynamics while increasing the force constants of all torsion angles
k_{NOE}: 50kcal/mol Å^2
k_{DIH}: from 1 to 200kcal/mol rad^2, increased by a factor of 1.30 per cycle
Step size: 0.5fs
Temperature: 1000K
d) 200 steps of minimization
e) Restrained molecular dynamics while cooling to 300K
28 cycles of 0.25ps each
Temperature increment: 25K per cycle
Step size: 0.5fs
f) 1000 steps of minimization

4) Refinement with dipolar couplings

Energy terms: bonds, angles, improper torsions, NOE, van der Waals (Lennard-Jones), electrostatic, dipolar
Switched van der Waals and electrostatic functions, with switching distances of 9.5 and 10.5Å, were used to truncate the number of possible interactions

a) 200 steps of minimization
k_{dipo} = 0.001kcal/mol Å^2
b) 15ps of restrained molecular dynamics
k_{dipo} : from 0.001 to 0.2kcal/mol Å^2, increased by a factor of 1.11 per cycle
Step size: 0.5fs
Temperature: 300K
c) 25ps of restrained molecular dynamics
Step size: 0.5fs
d) Analyze structures each 200 steps from 15ps to 25ps
e) 200 steps of minimization

Fig. 9. (*continued*)

mainly dipolar couplings and few NOE restraints. The authors measure ^{1}H–^{13}C, ^{1}H–^{15}N and ^{1}H–^{1}H residual dipolar couplings using samples in which complementary halves of the oligomer are isotopically labeled. ^{1}H–^{13}C and ^{1}H–^{15}N couplings were measured using HSQC experiments, and ^{1}H–^{1}H couplings were obtained from phase-sensitive COSY spectra. In a first step, starting structures are calculated from completely random structures. For this purpose only energy terms for bonds, angles and improper torsions are considered. In a second step, NOE and hydrogen bond restraints are included. The structures generated in this second step are refined against residual dipolar couplings in a series of molecular dynamic runs in which the dipolar force constants are increased slowly (Fig. 9). Again, it is not possible to obtain a good estimate of the magnitude and rhombicity of the alignment tensor on the basis of the dipolar coupling distribution, although it is possible to establish lower limits of the magnitude of the alignment. The optimum values are then derived from a grid search in which the dipolar energy term in the structure calculation is evaluated as a function of the magnitude and the rhombicity of the alignment.

The calculated dodecamer ensemble of structures are substantially different from the ones calculated without dipolar couplings and from previous NMR structures, but resemble those structures previously determined by X-ray crystallography (Fig. 10).

Recently, experiments designed to measure ^{1}H–^{31}P dipolar couplings have been reported [98,99]. This structural information can be very helpful in restraining the phosphodiester linkages that connect

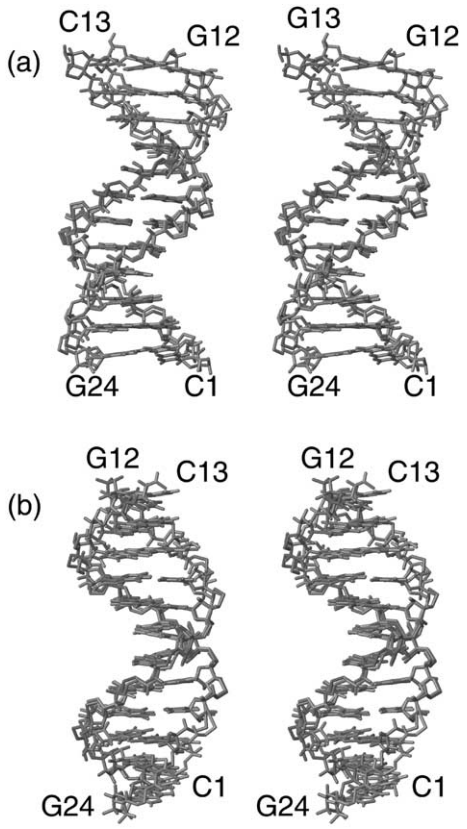

Fig. 10. Stereoviews of the NMR structure of a DNA dodecamer calculated using residual dipolar couplings. (a) and (b) differ in a 90° rotation around the helix axis to highlight the non-cylindrical symmetry of the molecule. These structures differ considerably from solution structures calculated without dipolar [97].

nucleotides in DNA and RNA. Nucleic acid backbone is usually poorly defined due to the difficulty in obtaining experimental restraints that depend on its conformation. This is the reason why $^{1}H-^{31}P$ dipolar couplings may have a special importance in the structure calculation of nucleic acids. Not only $^{1}H-^{31}P$ dipolar couplings but also ^{31}P CSA has been applied in the refinement of DNA (Fig. 11) demonstrating its usefulness in constraining the orientation of the phophodiester groups [100].

5.2. Dipolar couplings in the structure calculation of oligosaccharides

The conformational study of oligosaccharides is usually based on NOE and *J* coupling information combined with molecular modeling methods. Dipolar couplings have also been applied recently in the structure calculation of oligosaccharides. Aubin and Prestegard determined the conformation of a sialic acid attached to the surface of a magnetically oriented membrane-mimicking surface, on the basis of $^{1}H-^{13}C$ and $^{13}C-^{13}C$ dipolar couplings together with a single CSA induced shift [101]. A more recent example is reported in the work by Kiddle and Homans and concerns the application of residual $^{1}H-^{13}C$ dipolar couplings of a trisaccharide into a restrained dynamic simulated annealing protocol [102]. The authors demonstrate that it is possible to partially orient small molecules such as a trisaccharide in a dilute liquid crystalline medium. The value of the axial component of the alignment tensor is derived from the minimum dipolar coupling value, considering that the bond-vector having this value is aligned perpendicular to the principal axis of the tensor. The rhombic component instead, is derived from the usual minimization of the difference between the measured and the predicted dipolar couplings. Dipolar couplings restrain the conformation of the oligosaccharide better than regular short-range NOE data do, since the individual conformation of each monomer is fixed on the NMR time scale and motion in the molecule is a result of torsional oscillations about the glycosidic linkages.

$^{1}H-^{13}C$ dipolar couplings have also been used in the structure calculation of a pentasaccharide [103]. The molecule is considered as a rigid trisaccharide moiety whose conformation has been proposed previously. The dipolar coupling data provide

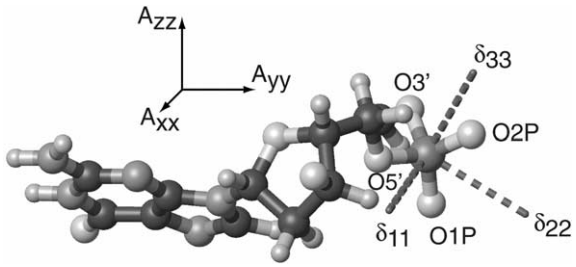

Fig. 11. ^{31}P CSA tensor orientation of a nucleotide from a DNA dodecamer with its helix axis pointing vertical. The DNA structure has been calculated using CSA data obtained under anisotropic conditions [100]. The CSA tensor is defined by δ_{11}, δ_{22}, δ_{33}. δ_{11} is orthogonal to the O1P–P–O2P plane. δ_{22} bisects the O1P–P–O2P angle. A_{xx}, A_{yy}, A_{zz} define the alignment tensor.

information concerning the conformation of the rest of the molecule and also agree with the proposed model for the trisaccharadide. The authors have evaluated in this work two methods for obtaining the orientation of the alignment tensor. One of the methods assumes that the alignment tensor is axially symmetric and considers that the order parameter S^2 as well as all H–C distances are equal for all C–H bonds. In the second method the tensor is considered asymmetric. The magnitude and orientation of the tensor are chosen such that they minimize the difference between the predicted and the measured dipolar coupling data. The authors conclude that both methods work fine in this case. The way to evaluate the agreement between the dipolar data and the proposed model for the trisaccharide moiety is based on the generation of dipolar maps in which the conformations with the minimum difference between the measured and the calculated dipolar couplings are represented. This strategy combined with the NOE data allows the authors to suggest that the linkage of the disaccharide with the rigid trisaccharide is of limited flexibility.

Additionally, ^{1}H–^{1}H dipolar couplings have been measured from COSY experiments in oriented oligosaccharides [104]. In the recent work reported by Martin–Pastor and Bush long-range ^{1}H–^{1}H and one-bond ^{13}C –^{1}H residual dipolar couplings are applied in the structure calculation of an heptasaccharide [105]. This work represents an example of the complexity of structure calculation in oligosaccharides, where conformational flexibility gives rise to incompatible NMR restraints. In the case of the heptasaccharide, residual dipolar couplings are incompatible due to the flexibility involved in glycosidic linkages. Thus, a unique alignment tensor cannot be determined. Nevertheless, as it occurs with the pentasaccharide, some dipolar couplings are useful in refining the more rigid moieties of the oligosaccharide.

As in the case of proteins or nucleic acids, the presence of flexibility and motion in oligosaccharides makes it more difficult to use dipolar coupling data in structure refinement. Conformational flexibility does not only imply that dipolar couplings are averaged but it is also possible that the different conformations can orient differently with respect to the magnetic field.

Acknowledgements

We would like to thank Dusty Baber, Ad Bax, Lewis E. Kay and Ben E. Ramirez for kindly providing some of the figures used in this manuscript. We are also very grateful to James A. Ferretti for the careful reading of the manuscript and useful suggestions.

References

[1] M. Karplus, J. Phys. Chem. 30 (1959) 11.
[2] S. Spera, A. Bax, J. Am. Chem. Soc. 113 (1991) 5490.
[3] D.S. Wishart, B.D. Sykes, F.M. Richards, J. Mol. Biol. 222 (1991) 311.
[4] A.J. Dingley, S. Grzesiek, J. Am. Chem. Soc. 120 (1998) 8293.
[5] K. Pervushin, A. Ono, C. Fernandez, T. Szyperski, M. Kainosho, K. Wuthrich, Proc. Natl. Acad. Sci. USA 95 (1998) 14147.
[6] Y.X. Wang, J. Jacob, F. Cordier, P. Wingfield, S.J. Stahl, S. Lee-Huang, D. Torchia, S. Grzesiek, A. Bax, J. Biomol. NMR 14 (1999) 181.
[7] N. Tjandra, Structure 7 (1999) R205.
[8] J.H. Prestegard, H.M. Al-Hashimi, J.R. Tolman, Q. Rev. Biophys. 33 (2000) 371.
[9] A. Bax, G. Kontaxis, N. Tjandra, Meth. Enzymol. 339 (2001) 127.
[10] A. Saupe, Angew. Chem., Int. Ed. Engl. 7 (1968) 97.
[11] J.W. Emsley, Liquid crystals: general considerations, in: D.M. Grant, R.K. Harris (Eds.), Encyclopedia of Nuclear Magnetic Resonance, 4, Wiley, Chichester, 1996.
[12] C. Gayathra, A.A. Bothner-By, P.C.M. van Zijl, C. MacLean, Chem. Phys. Lett. 87 (1982) 192.
[13] C.R. Sanders, J.P. Schwonek, Biochemistry 31 (1992) 8898.
[14] N. Tjandra, A. Bax, Science 278 (1997) 1111.
[15] J.R. Tolman, J.M. Flanagan, M.A. Kennedy, J.H. Prestegard, Proc. Natl. Acad. Sci. USA 92 (1995) 9279.
[16] M.A. Contreras, J. Ubach, O. Millet, J. Rizo, M. Pons, J. Am. Chem. Soc. 121 (1999) 8947.
[17] H.C. Kung, K.Y. Wang, I. Goljer, P.H. Bolton, J. Magn. Reson. B 109 (1995) 323.
[18] N. Tjandra, S. Grzesiek, A. Bax, J. Am. Chem. Soc. 118 (1996) 6264.
[19] G. Lipari, A. Szabo, J. Am. Chem. Soc. 104 (1982) 4546.
[20] B.E. Ramirez, A. Bax, J. Am. Chem. Soc. 120 (1998) 9106.
[21] N. Tjandra, J.G. Omichinski, A.M. Gronenborn, G.M. Clore, A. Bax, Nature Struct. Biol. 4 (1997) 732.
[22] M. Ottiger, A. Bax, J. Biomol. NMR 13 (1999) 187.
[23] G.M. Clore, D.S. Garret, J. Am. Chem. Soc. 121 (1999) 9008.
[24] E. de Alba, J.L. Baber, N. Tjandra, J. Am. Chem. Soc. 121 (1999) 4282.
[25] C.W. Hilbers, C. MacLean, Chem. Phys. Lett. 2 (1968) 445.
[26] M. Ottiger, A. Bax, J. Biomol. NMR 12 (1998) 361.

[27] J.A. Losonczi, J.H. Prestegard, J. Biomol. NMR 12 (1998) 447.
[28] S. Cavagnero, H.J. Dyson, P.E. Wright, J. Biomol. NMR 13 (1999) 387.
[29] R.S. Prosser, J.A. Losonczi, I.V. Shiyanovskaya, J. Am. Chem. Soc. 120 (1998) 11010.
[30] L.G. Barrientos, C. Dolan, A.M. Gronenborn, J. Biomol. NMR 16 (2000) 329.
[31] M. Ruckert, G. Otting, J. Am. Chem. Soc. 122 (2000) 7793.
[32] G.M. Clore, M.R. Starich, A.M. Gronenborn, J. Am. Chem. Soc. 120 (1998) 10571.
[33] M.R. Hansen, L. Mueller, A. Pardi, Nature Struct. Biol. 5 (1998) 1065.
[34] H.J. Sass, F. Cordier, A. Hoffmann, M. Rogowski, A. Cousin, J.G. Omichinski, H. Lowen, S. Grzesiek, J. Am. Chem. Soc. 121 (1999) 2047.
[35] B.W. Koenig, J.-S. Hu, M. Ottiger, S. Bose, R.W. Hendler, A. Bax, J. Am. Chem. Soc. 121 (1999) 1385.
[36] K. Fleming, D. Gray, S. Prasannan, S. Matthews, J. Am. Chem. Soc. 122 (2000) 5224.
[37] R. Tycko, F.J. Blanco, Y. Ishii, J. Am. Chem. Soc. 122 (2000) 9340.
[38] H.J. Sass, G. Musco, S.J. Stahl, P.T. Wingfield, S. Grzesiek, J. Biomol. NMR 18 (2000) 303.
[39] E. de Alba, L. De Vries, M. Farquhar, N. Tjandra, J. Mol. Biol. 291 (1999) 927.
[40] A. Bax, N. Tjandra, J. Biomol. NMR 10 (1997) 289.
[41] F. Delaglio, D. Torchia, A. Bax, J. Biomol. NMR 1 (1991) 439.
[42] C. Griesinger, O.W. Sorensen, R.R. Ernst, J. Magn. Reson. 75 (1987) 474.
[43] J.R. Tolman, J.H. Prestegard, J. Magn. Reson. B 112 (1996) 245.
[44] M. Ottiger, F. Delaglio, A. Bax, J. Magn. Reson. 131 (1998) 373.
[45] K. Pervushin, R. Riek, G. Wider, K. Wuthrich, Proc. Natl. Acad. Sci. USA 94 (1997) 12366.
[46] D.W. Yang, R.A. Venters, G.A. Mueller, W.Y. Choy, L.E. Kay, J. Biomol. NMR 14 (1999) 333.
[47] G. Kontaxis, G.M. Clore, A. Bax, J. Magn. Reson. 143 (2000) 184.
[48] P. Permi, A. Annila, J. Biomol. NMR 16 (2000) 221.
[49] P. Permi, P.R. Rosevear, A. Annila, J. Biomol. NMR 17 (2000) 43.
[50] E. de Alba, M. Suzuki, N. Tjandra, J. Biomol. NMR 19 (2001) 63.
[51] J.J. Chou, F. Delaglio, A. Bax, J. Biomol. NMR 18 (2000) 101.
[52] J. Santoro, G.C. King, J. Magn. Reson. 97 (1992) 202.
[53] M. Ottiger, F. Delaglio, J.L. Marquardt, N. Tjandra, A. Bax, J. Magn. Reson. 134 (1998) 365.
[54] M. Cai, H. Wang, E.T. Olejniczak, R.P. Meadows, A. Gunasekera, N. Xu, S.W. Fesik, J. Magn. Reson. 139 (1999) 451.
[55] F. Tian, J.A. Losonczi, M.W.F. Fischer, J.H. Prestegard, J. Biomol. NMR 15 (1999) 145.
[56] F. Tian, C.A. Fowler, E.R. Zartler, F.A.J. Jenney, M.W. Adams, J.H. Prestegard, J. Biomol. NMR 18 (2000) 23.
[57] G. Otting, M. Ruckert, M.H. Levitt, A. Moshref, J. Biomol. NMR 16 (2000) 343.
[58] M. Pellecchia, C.W. Vander Kooi, K. Keliikuli, E.R. Zuiderweg, J. Magn. Reson. 143 (2000) 435.
[59] T. Carlomagno, W. Peti, C. Griesinger, J. Biomol. NMR 17 (2000) 99.
[60] W. Peti, C. Griesinger, J. Am. Chem. Soc. 122 (2000) 343.
[61] G.M. Clore, A.M. Gronenborn, A. Bax, J. Magn. Reson. 131 (1998) 159.
[62] M. Zweckstetter, A. Bax, J. Am. Chem. Soc. 122 (2000) 3791.
[63] A.T. Brunger, XPLOR: A system for X-ray crystallography and NMR, 3.1 ed, Yale University Press, New Haven, 1993.
[64] J. Meiler, N. Blomberg, M. Nilges, C. Griesinger, J. Biomol. NMR 16 (2000) 245.
[65] J.A. Losonczi, M. Andrec, M.W.F. Fischer, J.H. Prestegard, J. Magn. Reson. 138 (1999) 334.
[66] N. Tjandra, J.L. Marquardt, G.M. Clore, J. Magn. Reson. 142 (2000) 393.
[67] F. Delaglio, G. Kontaxis, A. Bax, J. Am. Chem. Soc. 122 (2000) 2142.
[68] G.A. Mueller, W.Y. Choy, D. Yang, J.D. Forman-Kay, R.A. Venters, L.E. Kay, J. Mol. Biol. 300 (2000) 197.
[69] G.A. Mueller, W.Y. Choy, N.R. Skrynnikov, L.E. Kay, J. Biomol. NMR 18 (2000) 183.
[70] A.T. Brunger, Nature 355 (1992) 472.
[71] C. Gonzalez, J.A.C. Rullmann, A. Bonvin, R. Boelens, R. Kaptein, J. Magn. Reson. 91 (1991) 659.
[72] G.M. Clore, M.R. Starich, C.A. Bewley, M.L. Cai, J. Kuszewski, J. Am. Chem. Soc. 121 (1999) 6513.
[73] A.T. Brunger, G.M. Clore, A.M. Gronenborn, R. Saffrich, M. Nilges, Science 261 (1993) 328.
[74] G. Cornilescu, J.L. Marquardt, M. Ottiger, A. Bax, J. Am. Chem. Soc. 120 (1998) 6836.
[75] E. de Alba, N. Tjandra, J. Magn. Reson. 144 (2000) 367.
[76] R. Nikolai, N.R. Skrynnikov, L.E. Kay, J. Biomol. NMR 18 (2000) 239.
[77] M.A. Markus, R.B. Gerstner, D.E. Draper, D.A. Torchia, J. Mol. Biol. 292 (1999) 375.
[78] R.R. Biekofsky, F.W. Muskett, J.M. Schmidt, S.R. Martin, J.P. Browne, P.M. Bayley, J. Feeney, FEBS Lett. 460 (1999) 519.
[79] N.R. Skrynnikov, N.K. Goto, D. Yang, W.-Y. Choy, J.R. Tolman, G.A. Mueller, L.E. Kay, J. Mol. Biol. 295 (2000) 1265.
[80] N.K. Goto, N.R. Skrynnikov, F.W. Dahlquist, L.E. Kay, J. Mol. Biol. 308 (2001) 745.
[81] M.W.F. Fischer, J.A. Losonczi, J. Lim Weaver, J.H. Prestegard, Biochemistry 38 (1999) 9013.
[82] P.J. Bolon, H.M. Al-Hashimi, J.H. Prestegard, J. Mol. Biol. 293 (1999) 107.
[83] B.W. Koenig, D.C. Mitchell, S. Konig, S. Grzesiek, B.J. Litman, A. Bax, J. Biomol. NMR 16 (2000) 121.
[84] J.-C. Hus, D. Marion, M. Blackledge, J. Mol. Biol. 298 (2000) 921.
[85] G.M. Clore, Proc. Natl. Acad. Sci. USA 97 (2000) 9021.
[86] A. Annila, H. Aitio, E. Thulin, T. Drakenberg, J. Biomol. NMR 14 (1999) 223.

[87] J. Meiler, W. Peti, C. Griesinger, J. Biomol. NMR 17 (2000) 283.
[88] C.A. Fowler, F. Tian, H.M. Al-Hashimi, J.H. Prestegard, J. Mol. Biol. 304 (2000) 447.
[89] J.J. Chou, S. Li, A. Bax, J. Biomol. NMR 18 (2000) 217.
[90] H. Zhou, A. Vermeulen, F.M. Jucker, A. Pardi, Biopolymers 52 (1999) 168.
[91] E.T. Mollova, A. Pardi, Curr. Opin. Struct. Biol. 10 (2000) 298.
[92] P. Bayer, L. Varani, G. Varani, J. Biomol. NMR 14 (1999) 149.
[93] A. Ramos, S. Grunert, J. Adams, D.R. Micklem, M.R. Proctor, S. Freund, M. Bycroft, D. St Johnson, G. Varani, EMBO J. 19 (2000) 997.
[94] S.R. Lynch, J.D. Puglisi, J. Am. Chem. Soc. 122 (2000) 7853.
[95] D. MacDonald, K. Herbert, X. Zhang, T. Polgruto, P. Lu, J. Mol. Biol. 306 (2001) 1081.
[96] R.D. Beger, V.M. Marathias, B.F. Volkman, P.H. Bolton, J. Magn. Reson. 135 (1998) 256.
[97] N. Tjandra, S.-i. Tate, A. Ono, M. Kainosho, A. Bax, J. Am. Chem. Soc. 122 (2000) 6190.
[98] M. Hennig, T. Carlomagno, J.R. Williamson, J. Am. Chem. Soc. 123 (2001) 3395.
[99] Z. Wu, N. Tjandra, A. Bax, J. Biomol. NMR 19 (2001) 367.
[100] Z. Wu, N. Tjandra, A. Bax, J. Am. Chem. Soc. 123 (2001) 3617.
[101] Y. Aubin, J.H. Prestegard, Biochemistry 32 (1993) 3422.
[102] G.R. Kiddle, S.W. Homans, FEBS Lett. 436 (1998) 128.
[103] M. Martin-Pastor, C.A. Bush, Carbohydr. Res. 323 (2000) 147.
[104] P.J. Bolon, J.H. Prestegard, J. Am. Chem. Soc. 120 (1998) 9366.
[105] M. Martin-Pastor, C.A. Bush, J. Biomol. NMR 19 (2001) 125.
[106] M. Piotto, V. Saudek, V. Sklenar, J. Biomol. NMR 2 (1992) 661.
[107] D. Marion, M. Ikura, R. Tschudin, A. Bax, J. Magn. Reson. 85 (1989) 393.
[108] N.N. Dewji, D.A. Wenger, S. Fujibayashi, M. Donoviel, F. Esch, F. Hill, J.S. O'Brien, Biochem. Biophys. Res. Commun. 134 (1986) 989.
[109] J.L. Baber, D. Libutti, D. Levens, N. Tjandra, J. Mol. Biol. 289 (1999) 949.